Infectious Disease Modelling 9 (2024) 1007–1026

Contents lists available at ScienceDirect

Infectious Disease Modelling

journal homepage: www.keaipublishing.com/idm

Modeling measles transmission in adults and children: Implications to vaccination for eradication

Anjana Pokharel [a, b], Khagendra Adhikari [b, c], Ramesh Gautam [b, d], Kedar Nath Uprety [b, e], Naveen K. Vaidya [b, f, g, h, *]

[a] Padma Kanya Multiple Campus, Tribhuvan University, Kathmandu, Nepal
[b] Mathematical Biology Research Center, Kathmandu, Nepal
[c] Amrit Campus, Tribhuvan University, Kathmandu, Nepal
[d] Ratna Rajya Laxmi Campus, Tribhuvan University, Kathmandu, Nepal
[e] Central Department of Mathematics, Tribhuvan University, Kathmandu, Nepal
[f] Department of Mathematics and Statistics, San Diego State University, San Diego, CA, USA
[g] Computational Science Research Center, San Diego State University, San Diego, CA, USA
[h] Viral Information Institute, San Diego State University, San Diego, CA, USA

ARTICLE INFO

Article history:
Received 2 February 2024
Received in revised form 17 April 2024
Accepted 29 April 2024
Available online 4 May 2024
Handling Editor: Dr. Raluca Eftimie

2010 MSC:
34K20
34L30
92B05
92D30

Keywords:
Measles eradication
Measles reservoir
Adult-child vaccination
Adults and children groups
Nepal

ABSTRACT

Despite the availability of successful vaccines, measles outbreaks have occurred frequently in recent years, presumably due to the lack of proper vaccination implementation. Moreover, measles cases in adult groups, albeit small in number, indicate that the previously neglected adult group may need to be brought into vaccine coverage to achieve WHO's goal of measles eradication from the globe. In this study, we develop a novel transmission dynamics model to describe measles cases in adults and children to evaluate the role of adult infection in persistent measles cases and vaccination programs for eradication. Analysis of our model, validated by measles cases from outbreaks in Nepal, provides the vaccination reproduction number (conditions for measles eradication or persistence) and the role of contact network size. Our results highlight that while children are primary targets for measles outbreaks, a small number of infections in adults may act as a reservoir for measles, causing obstacles to eradication. Furthermore, our model analysis shows that while impactful controls can be achieved by children-focused vaccines, a combined adult-child vaccination program may help assert eradication of the disease.

1. Introduction

Measles, a disease caused by the morbillivirus, remains a major global health concern. Despite the availability of effective vaccines, measles outbreaks occur frequently, especially among children, and the infection causes severe complications in infected individuals. According to WHO, measles vaccination averted around 56 million deaths due to this disease during the 21-year time (between 2000 and 2021) (WHO, 2023a). However, in 2021, there were 128,000 recorded deaths due to measles, occurring primarily among unvaccinated or partially vaccinated children, highlighting the need for more focused prevention efforts to bring the global measles cases down (WHO, 2023a).

* Corresponding author. Mathematical Biology Research Center, Kathmandu, Nepal.
E-mail address: nvaidya@sdsu.edu (N.K. Vaidya).
Peer review under responsibility of KeAi Communications Co., Ltd.

https://doi.org/10.1016/j.idm.2024.04.012

Various factors, including limited access to healthcare systems, vaccine hesitancy driven by skepticism, and the impact of the COVID-19 pandemic on vaccine coverage, have collectively hampered vaccination programs in 2021. In 2021, a record high of nearly 40 million children missed a measles vaccine dose; 25 million children missed their first dose, and an additional 14.7 million children missed their second dose (WHO, 2022). The world data is well under that, with only 81% of children receiving their first measles-containing vaccine dose, and only 71% of children receiving their second one. Note that the World Health Organization (WHO) recommends at least 95 percent vaccination coverage to achieve herd immunity for measles (Unicef for Every Child, 2019).

The decline in vaccine coverage coincides with measles transmission patterns, impacting not only infants but also older age groups (Meredith et al., 2021). Major challenges for measles control include a lack of a catch-up vaccination program, growing vaccine hesitancy, and insufficient monitoring for elimination and outbreak prevention. In response, the World Health Organization introduced the "Measles and Rubella Strategic Framework 2021–2030" in 2020, targeting global disease elimination by 2030 (WHO, 2020; WHO, 2023a).

In Nepal, measles vaccination was introduced in 1979, but until 2007, national MCV1 coverage remained below 85 percent, resulting in childhood mortality due to measles. From 2007 to 2014, MCV1 coverage increased from 81% in 2007 to 88% in 2014 (WHO, 2023b). As a result, a remarkable reduction of 98% in measles cases was achieved by 2017 (Sekhar et al., 2022). However, the cases rose in 2018–2019 by 66% (from 260 to 431) (WHO, 2023c). In response, the National Immunization Program (NIP) was introduced in 2020 with a plan for a comprehensive nationwide vaccination campaign targeting children aged 9–59 months against both measles and rubella (MR). While the first phase of this campaign was completed as scheduled, the second phase was disrupted by the COVID-19 pandemic, consequently causing measles outbreaks in multiple districts (Sekhar et al., 2022; Thakur et al., 2024). Between January and April 2020, 220 measles cases were reported, with 78% affecting individuals outside the campaign's target age range (9–59 months). Notably, 60% of the total cases in the 5–14 year age group were not vaccinated (Sekhar et al., 2022).

Recently, from November 2022 to March 2023, 690 cases were reported, with approximately 86% of infected individuals aged 15 years and younger, and 58% of the patients were unvaccinated (WHO, 2023d). While a rising number of measles cases has brought attention to the potential threat of severe measles outbreaks, persistent and frequent outbreaks in specific districts, including Morang, Dang, Kapilvastu, Kathmandu, Lalitpur, Dhading, Banke, Kailali, of Nepal pose a severe concern of obstacle to World Health Organisation's (WHO's) global measles eradication plan "Measles and Rubella Strategic Framework 2021–2030" (Dall, 2023; Poudel, 2019; WHO, 2020; WHO, 2023a; WHO, 2023d). In order to achieve the measles eradication goal, the primary focus has been on formulating improved children-vaccination programs. However, it is essential to note that 14% of the infectious cases are unvaccinated adults. Notably, these infectious adults originating from the pool of unvaccinated children can act as virus reservoirs in the community and sources for disease outbreaks, despite the control in the children group, causing the obstacle to disease eradication. Therefore, implementing a closely monitored vaccination program combined for both children and adults may be imperative to devise a program for completely eradicating the disease.

Mathematical models play a vital role in understanding transmission dynamics, forecasting outbreaks, and proposing effective control strategies (Adhikari et al., 2021; Adhikari et al., 2022; Gautam et al., 2022; Mutua, Wang, & Vaidya, 2015; Vaidya & Wang, 2022). Therefore, mathematical modeling can be a valuable tool for studying measles transmission in children and adult subgroups with different degrees of interactions between intragroup and intergroup populations residing in the same community. Numerous mathematical models have been developed for measles, including SIR, SEIR, SVEIR and SVEIRS, SVEIHR, fractional derivative models, to explore various aspects of measles dynamics (Edward et al., 2015; Farman et al., 2023; Haileyesus & Asnakew, 2023; Kuddus et al., 2021; Peter et al., 2022, 2023a, 2023b; Roberts, 2000; Song et al., 2019; Trottier & Philippe, 2000). Specifically in the context of Nepal, previous studies have discussed progress in measles control, case fatality rates, and the genetic type of the Asian measles virus, most incorporating vaccination (Joshi, 2009; Khanal, 2016; Poudel, 2019; Truong et al., 2001). In Pokharel et al. (2022), we introduced a deterministic model to examine the effect of monitored and un-monitored vaccination in children of Nepal (Pokharel et al., 2022). However, none of the previous models has considered the adult group, presumably the critical group for the global eradication of measles.

In this study, we consider measles cases in adults, a more mobile critical group typically not included in regular immunization programs. We introduce a novel deterministic model, incorporating monitored vaccination for children and adults to assess the impact of these adult-child vaccination approaches on measles eradication in Nepal. The model is validated using fifteen weeks of measles data from Nepal. Our model analysis evaluates the local and global stability of disease-free equilibrium and the existence of at least one endemic equilibrium. We simulate our model to assess the impact of monitored adult-child vaccination programs on reducing measles transmission in Nepal and eventually eradicating the disease over a period of time.

2. Model formulation

2.1. Data source

The publicly available data used in this work is obtained from the official website of the World Health Organization (WHO) (WHO-Nepal, 2023a). From November 24, 2022, to March 10, 2023, a total of 690 cases of measles were recorded in western Nepal, spanning outbreaks in seven districts: Banke (327 cases), Surkhet (62 cases), Bardiya (49 cases), Kailali (39 cases), Kanchanpur (27 cases), Bajura (13 cases), and Dang (12 cases). Additionally, three districts in eastern Nepal also reported

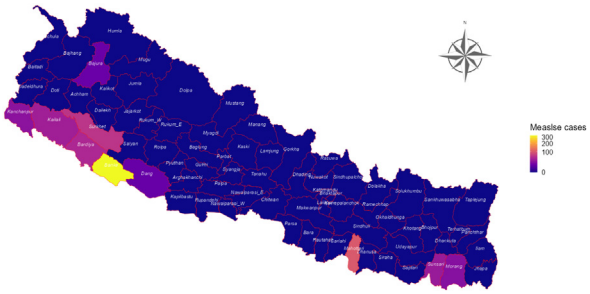

Fig. 1. Measles Cases in Nepal. Measles cases in different parts of Nepal from November 24, 2022, to March 10, 2023. The map was created using the cartography package in R 4.3.1.

cases: Mahottari (103 cases), Sunsari (34 cases), and Morang (24 cases). The distribution of measles cases is shown in Fig. 1. Among these reported cases, one death was reported, indicating a Case Fatality Rate (CFR) of 0.14% (Dall, 2023).

2.2. Transmission dynamics model

We categorize the population into two different age groups (0–15 yrs and above 15 yrs) based on the data (Dall, 2023) and develop a deterministic mathematical model ($SVEII_m$) to describe the transmission dynamics of measles among those two groups. Since measles can be prevented by complete doses of vaccines and individuals gain lifelong immunity after recovery from infection (Edward et al., 2015), we do not consider re-infection in our model. The indices C and A represent the child (0–15 yrs) and adult (above 15) groups, respectively. The group of children and adults are divided into six distinct compartments $(S_C,\ U_C^V,\ M_C^V,\ E_C,\ I_C,\ I_{mC})$ and $(S_A,\ U_A^V,\ V_A,\ E_A,\ I_A,\ I_{mA})$, respectively, as shown in Fig. 2. Λ is the recruitment rate of newborns, and ψ is the maturation rate of a child becoming an adult.

Building an effective vaccination program is often difficult, especially when parents lack adequate health knowledge and are skeptical about vaccines. One way to improve the efficacy of immunization is to incorporate a monitored vaccination program so that children who signed up for it receive their immunizations accurately and on time. The unmonitored class includes children not enrolled in the monitored program. The children in this class may frequently skip the complete vaccine doses on time, presumably due to the lack of parents' health consciousness and/or the lack of supervision for proper immunization. On the other hand, the monitored class includes the children enrolled in the monitored program, which ensures enrolled members with supervision for timely immunization of complete doses. Our objective in this study is to develop a model to evaluate such monitored vaccination programs for controlling measles in both children and adults, with the goal of eradicating measles.

In this context, we assume children engaged in the monitored vaccination program exhibit a lower vulnerability to diseases and a greater probability of acquiring immunity due to increased attention and regular supervision, in contrast to children under unsupervised immunization schemes. Consequently, the children eligible for vaccination are divided into two distinct groups: the Un-monitored Vaccination Group (U_A^V), consisting of vaccinated children undergoing routine vaccination without supervision, and the Monitored Vaccination Group (M_C^V), comprising children vaccinated under supervision to

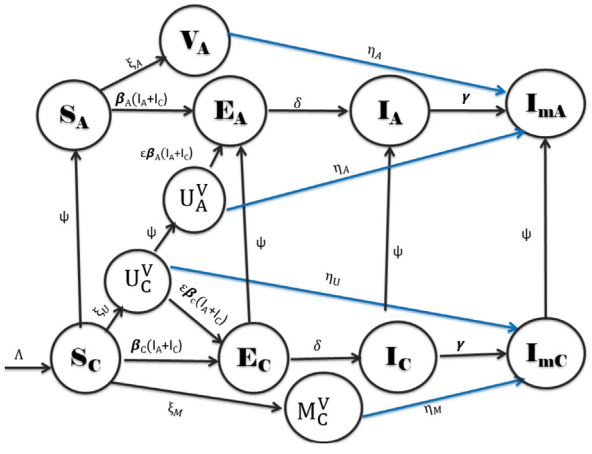

Fig. 2. Schematic diagram of the model: The group of children is divided into six distinct compartments: S_C (Susceptible), U_C^V (Un-monitored Vaccinated), M_C^V (Monitored Vaccinated), E_C (Exposed), I_C (Infectious), and I_{mC} (Immune). Similarly, the adult age group is divided into six subgroups $(S_A,\ U_A^V, V_A,\ E_A,\ I_A,\ I_{mA})$.

Table 1
Description of the parameters.

Symbols	Description
Λ	Recruitment rate to children group
ξ_U, ξ_M	Un-monitored and Monitored children Vaccination rate
ξ_A	Adult Vaccination rate
β_C, β_A	Transmission rate on the children and adults
μ	Natural death rate
γ	Rate of being immune after recovery from infection
ψ	Maturation rate
$(1-\epsilon)$	Effectiveness of the vaccination
η_A	Rate of being immune of Un-monitored vaccinated adults
η_U, η_M	Rate of being immune of Un-monitored, Monitored vaccinated children
δ	Incubation period
d	Disease induced death

ensure timely administration. In addition, we consider the Adult Vaccination Group (V_A), which consists of vaccinated adults under supervision through the catch-up vaccination program.

Upon successfully receiving both vaccine doses per the recommended schedule, we assume that the Monitored Vaccination Group and Adult Vaccination Group will attain sufficient immunization and become non-susceptible to diseases. η_M and η_A represent the rate of immunization of the Monitored Vaccination Group and Adult Vaccination Group, respectively, and β_C represents the rate of the fully susceptible children becoming infected.

Given the possibility of incomplete administration of vaccine doses within the Un-monitored Vaccination Group, there remains a potential susceptibility to diseases. To capture this infection, we account for disease transmission within this group at a rate of $\epsilon\beta_C$, where $(1-\epsilon)$ represents the vaccine's effectiveness. Additionally, we consider a different infection rate, denoted by β_A, for the adult group, assuming that measles transmission is low among adults. The complete description of the parameters is given in Table 1.

The equations of the dynamical system describing measles transmission are as follows:

$$\frac{dS_C}{dt} = \Lambda - (\mu + \xi_M + \xi_U + \psi)S_C - \beta_C(I_C + I_A)S_C, \tag{1}$$

$$\frac{dS_A}{dt} = \psi\ S_C - \beta_A(I_C + I_A)S_A - \mu\ S_A - \xi_A S_A, \tag{2}$$

$$\frac{dU_C^V}{dt} = \xi_U\ S_C - \epsilon\beta_C(I_C + I_A)U_C^V - (\mu + \eta_U + \psi)U_C^V, \tag{3}$$

$$\frac{dU_A^V}{dt} = \psi U_C^V - \eta_A U_A^V - \beta_A\epsilon(I_C + I_A)U_A^V - \mu U_A^V, \tag{4}$$

$$\frac{dV_A}{dt} = \xi_A S_A - V_A(\mu + \eta_A), \tag{5}$$

$$\frac{dM_C^V}{dt} = \xi_M S_C - (\mu + \eta_M)M_C^V, \tag{6}$$

$$\frac{dE_C}{dt} = \beta_C(I_C + I_A)S_C + \beta_C\epsilon(I_C + I_A)U_C^V - (\delta + \mu + \psi)E_C, \tag{7}$$

$$\frac{dE_A}{dt} = \beta_A(I_C + I_A)S_A + \beta_A\epsilon(I_C + I_A)U_A^V + \psi E_C - (\delta + \mu)E_A, \tag{8}$$

$$\frac{dI_C}{dt} = \delta E_C - (\gamma + d + \mu + \psi)I_C, \tag{9}$$

$$\frac{dI_A}{dt} = \delta E_A + \psi E_C - (\gamma + d + \mu)I_A, \tag{10}$$

$$\frac{dI_{mC}}{dt} = \gamma I_C + \eta_M M_C^V - (\mu + \psi)I_{mC} + \eta_U U_C^V, \tag{11}$$

$$\frac{dI_{mA}}{dt} = \eta_A(U_A^V + V_A) + \gamma I_A - \mu I_{mA} + \psi I_{mC}. \tag{12}$$

3. Model analysis

3.1. Positivity and boundedness of the solutions

In the system (1–12), all the state variables are non-negative and should remain non-negative forever since they represent the human population. For the given non-negative initial conditions, it can be easily verified that system (1-12) has non-negative solutions at any time t as shown in the following theorem.

Theorem 3.1. *If the state variable are non-negative with $S_C > 0$ at time $t = 0$, then the solution set of the system (1 - 12) is always non-negative and bounded.*

Proof:
First, we prove that all the solutions are non-negative. From the system (1–12), we get

$$\begin{aligned}
\frac{dS_C}{dt} &= \Lambda - (\mu + \xi_M + \xi_U + \psi)S_C - \beta_C(I_C + I_A)S_C \\
&> -(\mu + \xi_M + \xi_U + \psi)S_C - \beta_C(I_C + I_A)S_C \\
\Rightarrow S_C &> S_C(0)\exp\left(- \int_0^t ((\mu + \xi_M + \xi_U + \psi) + \beta_C(I_C + I_A))\, dt \right) \geq 0; \\
\frac{dS_A}{dt} &= \psi\, S_C - \beta_A(I_C + I_A)S_A - \mu\, S_A - \xi_A\, S_A \\
&> -\beta_A(I_C + I_A)S_A - \mu\, S_A - \xi_A S_A \\
\Rightarrow S_A &> S_A(0)\exp\left(- \int_0^t \beta_A((I_C + I_A) + \mu + \xi_A)\, dt \right) > 0; \\
\frac{dU_C^V}{dt} &= \xi_U\, S_C - \beta_C\, \epsilon(I_C + I_A)U_C^V\ - (\mu + \eta_U + \psi)U_C^V \\
&> -\beta_C\, \epsilon\, (I_C + I_A)U_C^V - (\mu + \eta_U + \psi)U_C^V \\
\Rightarrow U_C^V &\geq U_C^V(0)\exp\beta_C\epsilon\left(- \int_0^t ((I_C + I_A) + (\mu + \eta_U + \psi))\, dt \right) \geq 0; \\
\frac{dU_A^V}{dt} &= \psi\, U_C^V - \eta_A\, U_A^V - \beta_A\, \epsilon(I_C + I_A)U_A^V - \mu\, U_A^V \\
&> -\eta_A\, U_A^V - \beta_A\, \epsilon\, (I_C + I_A)U_A^V - \mu\, U_A^V \\
\Rightarrow U_A^V &\geq U_A^V(0)\exp\left(- \int_0^t \beta_A\, \epsilon\, (\eta_A + (I_C + I_A) + \mu)\, dt \right) \geq 0; \\
\frac{dV_A}{dt} &= \xi_A S_A - V_A(\mu + \eta_A) > -V_A(\mu + \eta_A) \\
\Rightarrow V_A &> V_A(0)\exp\left(- \int_0^t (\eta_A + \mu)\, dt \right) \geq 0; \\
\frac{dM_C^V}{dt} &= \xi_M\, S_C - (\mu + \eta_M)M_C^V \\
&> -(\mu + \eta_M)M_C^V \\
\Rightarrow M_C^V &\geq M_C^V(0)\exp\left(- \int_0^t ((\mu + \eta_M))\, dt \right) \geq 0; \\
\text{and } \frac{dE_C}{dt} &= \beta_C(I_C + I_A)S_C + \beta_A\, \epsilon(I_C + I_A)U_C^V - (\delta + \mu + \psi)E_C \\
&\geq -((\delta + \mu + \psi))E_C \\
\Rightarrow E_C &\geq E_C(0)\exp\left(- \int_0^t ((\delta + \mu + \psi))\, dt \right) \geq 0.
\end{aligned}$$

Similarly, $E_A, I_C, I_A, I_{mC}, I_{mA}$ are also non-negative. Hence, the solution set $\{S_C, S_A, U_C^V, U_A^V, V_A, M_C^V, E_C, E_A, I_C, I_A, I_{mC}, I_{mA}\}$ of system (1–12) is always non-negative.

We now prove that these non-negative solutions are bounded. Let $N_h(t)$ be the total human population, i.e., $N_h(t) = S_C(t) + S_A(t) + U_C^V(t) + U_A^V(t) + V_A(t) + M_C^V(t) + E_C(t) + E_A(t) + I_C(t) + I_A(t) + I_{mC}(t) + I_{mA}(t)$. Adding all the equations of the system (1–12), we obtain

$$\frac{dN_h}{dt} = \Lambda - \mu N_h - d(I_C + I_A) \leq \Lambda - \mu N_h,$$

which implies

$$\lim_{t\to\infty} N_h \leq \Lambda/\mu.$$

Hence, the human population, $N_h(t)$, is ultimately bounded.

Using the above conditions, we have that for any $\alpha > 0$, there exists $t_\alpha > 0$ such that the solution of the system with $t \geq t_\alpha$ lies in the compact set $\Omega = \Omega_h$, where $\Omega_h = \left\{ \left(S_C, S_A, U_C^V, U_A^V, V_A, M_C^V, E_C, E_A, I_C, I_A, I_{mC}, I_{mA}\right) \in \Re_+^{12} : N_h \leq \Lambda/\mu + \alpha \right\}$. Thus, all the state variables representing the populations are non-negative and bounded.

3.2. Disease-free equilibrium and reproduction number

Here, we derive the expression of the disease-free and endemic equilibrium points. Taking $E_C^0 = 0$, $E_A^0 = 0$, $I_C^0 = 0$, $I_A^0 = 0$, we obtain the disease-free equilibrium: $E^0 = (S_C^0,\ S_A^0,\ (U_C^V)^0,\ (U_A^V)^0, V_A^0,\ (M_C^V)^0,\ 0,\ 0,\ 0,\ 0,\ I_{mC}^0,\ I_{mA}^0)$, where

$$\begin{aligned}
S_C^0 &= \frac{\Lambda}{\mu + \xi_M + \xi_U + \psi},\\
S_A^0 &= \frac{\Lambda\psi}{(\xi_A + \mu)(\mu + \xi_M + \xi_U + \psi)},\\
\left(U_C^V\right)^0 &= \frac{\Lambda\xi_U}{Z(\mu + \xi_M + \xi_U + \psi)},\\
\left(U_A^V\right)^0 &= \frac{\Lambda\psi\xi_U}{Z(\eta_A + \mu)(\mu + \xi_M + \xi_U + \psi)},\\
V_A^0 &= \frac{\Lambda\psi\xi_A}{(\eta_A + \mu)(\xi_A + \mu)(\mu + \xi_M + \xi_U + \psi)},\\
\left(M_C^V\right)^0 &= \frac{\Lambda\xi_M}{Z_1(\mu + \xi_M + \xi_U + \psi)},\\
I_{mC}^0 &= \frac{\Lambda(\eta_M(\xi_M Z + \eta_U\xi_U) + \mu\eta_U\xi_U)}{ZZ_1(\mu + \psi)(\mu + \xi_M + \xi_U + \psi)},\\
I_{mA}^0 &= \frac{\Lambda\psi\left(ZZ_1\eta_A(\xi_A(\mu + \psi) + \mu(Z_1\xi_M + \eta_M\xi_U)) + \mu^2(Z_1\eta_U\xi_U + Z\eta_M\xi_M)\right)}{ZZ_1\mu^2(\mu + \psi)(\eta_A + \mu)(\mu + \xi_M + \xi_U + \psi)},\\
\text{and } Z &= (\mu + \eta_U + \psi),\ Z_1 = (\mu + \eta_M).
\end{aligned}$$

Given that a significant portion of the population has already been vaccinated, we adopt a similar approach to our previous study (Pokharel et al., 2022) in defining the vaccinated reproduction number, R_v. This is done considering the presence of the vaccinated population, as opposed to an entire population susceptible to infection. The vaccinated reproduction number, R_v, represents the average number of secondary cases resulting from introducing a single infectious case into the mixed population, which comprises individuals with both susceptible and vaccinated status. To calculate R_v, we utilize the Next Generation Matrix method described in previous studies (Diekmann & Heesterbeek, 2001; van den Driessche & Watmough, 2002; Diekmann, Heesterbeek, & Roberts, 1992).

Following the Next Generation Matrix method (van den Driessche & Watmough, 2002), we divide the system into two groups, infected $\vec{x} = (x_i, i = 1, 2, 3, 4) = (E_C,\ E_A,\ I_C,\ I_A)$ and uninfected $\vec{y} = (y_j, j = 1,2,3,4,5,6,7,8) = (S_C,\ S_A,\ U_C^V,\ U_A^V,\ V_A,\ M_C^V,\ I_{mC},\ I_{mA})$. We then set $\dot{x}_i = f_i(\vec{x}, \vec{y}) = \mathcal{F}_i(x,y) - \mathcal{V}_i(x,y)$ for $i = 1, 2..4$ and $\dot{y}_j = g_j(\vec{x}, \vec{y})$ for $j = 1, 2 \ldots, 8$, where $\mathcal{F}_i(x,y)$ is the rate of appearance of new infections in the compartment i and $\mathcal{V}_i(x,y)$ is the difference between the transfer of individuals out of and into the compartment i for $i = 1, 2, 3, 4$. Here we have

$$\mathcal{F} = \begin{pmatrix} \beta_C(I_C + I_A)S_C + (I_C + I_A)\beta_C U_C^V \epsilon \\ \beta_A(I_C + I_A)S_A + (I_C + I_A)\beta_A U_A^V \epsilon \\ 0 \\ 0 \end{pmatrix} \text{ and } \mathcal{V} = \begin{pmatrix} (\delta + \mu + \psi)E_C \\ -E_C\psi + E_A(\delta + \mu) \\ -E_C\delta + I_C(\gamma + d + \mu + \psi) \\ -E_A\delta - I_C\psi + I_A(\gamma + d + \mu) \end{pmatrix}.$$

It is straightforward to confirm that the conditions A(1)-A(5) mentioned in van den Driessche & Watmough (2002) are satisfied by the sets $\mathcal{F}_i$ and $\mathcal{V}_i$ for $i = 1, 2, 3, 4$. We derive the Jacobian matrices of $\mathcal{F}$ and $\mathcal{V}$ at disease-free equilibrium point (E^0), yielding $D\mathcal{F}(E^0) = F$ and $D\mathcal{V}(E^0) = V$ as follows:

$$F = \begin{pmatrix} 0 & 0 & \beta_C S_C^0 + \beta_C (U_C^V)^0 \epsilon & \beta_C S_C^0 + \beta_C (U_C^V)^0 \epsilon \\ 0 & 0 & \beta_A S_A^0 + \beta_A (U_A^V)^0 \epsilon & \beta_A S_A^0 + \beta_A (U_A^V)^0 \epsilon \\ 0 & 0 & 0 & 0 \\ 0 & 0 & 0 & 0 \end{pmatrix},$$

$$V = \begin{pmatrix} \delta + \mu + \psi & 0 & 0 & 0 \\ -\psi & \delta + \mu & 0 & 0 \\ -\delta & 0 & \gamma + d + \mu + \psi & 0 \\ 0 & -\delta & -\psi & \gamma + d + \mu \end{pmatrix},$$

$$V^{-1} = \begin{pmatrix} \frac{1}{\delta + \mu + \psi} & 0 & 0 & 0 \\ \frac{\psi}{(\delta + \mu)(\delta + \mu + \psi)} & \frac{1}{\delta + \mu} & 0 & 0 \\ \frac{\delta^2 + \delta\mu}{L} & 0 & \frac{1}{\gamma + d + \mu + \psi} & 0 \\ \frac{\delta\psi(\gamma + \delta + d + 2\mu + \psi)}{L(\gamma + d + \mu)} & \frac{\delta}{(\delta + \mu)(\gamma + d + \mu)} & \frac{\psi}{(\gamma + d + \mu)(\gamma + d + \mu + \psi)} & \frac{1}{\gamma + d + \mu} \end{pmatrix},$$

where $L = (\delta + \mu)(\delta + \mu + \psi)(\gamma + d + \mu + \psi)$. Since F is a non-negative and V is a non-singular M-matrix, the next generation matrix FV^{-1} exists, and its spectral radius $\rho(FV^{-1})$ gives the vaccinated reproduction number R_v. Therefore,

$$R_v = \frac{\delta\left(\beta_C S_C^0 + \beta_A S_A^0 + \epsilon\beta_C (U_C^V)^0 + \epsilon\beta_A (U_A^V)^0\right)}{(\delta + \mu)(\gamma + d + \mu)}$$

$$= \frac{\delta\Lambda(\beta_C\epsilon\xi_U(\eta_A + \mu)(\xi_A + \mu) + \beta_A\psi\epsilon\xi_U(\xi_A + \mu) + \beta_C Z(\eta_A + \mu)(\xi_A + \mu) + \beta_A\psi Z(\eta_A + \mu))}{Z(\delta + \mu)(\eta_A + \mu)(\xi_A + \mu)(\gamma + d + \mu)(\mu + \xi_M + \xi_U + \psi)}.$$

We also compute the time-dependent effective reproduction number, denoted by R_e. The R_e value aids us in monitoring whether the epidemic at a given time t is exhibiting an upward trend ($R_e > 1$) or a downward trend ($R_e < 1$). In our model, the effective reproduction number is determined by the following expression:

$$R_e = \frac{\delta\left(\beta_C S_C(t) + \beta_A S_A(t) + \epsilon\beta_C U_C^V(t) + \epsilon\beta_A U_A^V(t)\right)}{(\delta + \mu)(\gamma + d + \mu)}.$$

3.3. Stability of disease free equilibrium E^0

3.3.1. Local stability of disease free equilibrium E^0

The Jacobian J_0 of the system (1–12) at the disease free equilibrium E^0 is given by $J_0 = [A_{12\times 6}\ B_{12\times 6}]$, where

$$A_{12\times 6}=\begin{pmatrix} -\mu-\xi_M-\xi_U-\psi & 0 & 0 & 0 & 0 & 0\\ \psi & -\mu-\xi_A & 0 & 0 & 0 & 0\\ \xi_U & 0 & -\mu-\eta_U-\psi & 0 & 0 & 0\\ 0 & 0 & \psi & -\eta_A-\mu & 0 & 0\\ 0 & \xi_A & 0 & 0 & -\eta_A-\mu & 0\\ \xi_M & 0 & 0 & 0 & 0 & -\mu-\eta_M\\ 0 & 0 & 0 & 0 & 0 & 0\\ 0 & 0 & 0 & 0 & 0 & 0\\ 0 & 0 & 0 & 0 & 0 & 0\\ 0 & 0 & 0 & 0 & 0 & 0\\ 0 & 0 & \eta_U & 0 & 0 & \eta_M\\ 0 & 0 & 0 & \eta_A & \eta_A & 0 \end{pmatrix},$$

$$B_{12\times 6}=\begin{pmatrix} 0 & 0 & -\beta_C S_C & -\beta_C S_C & 0 & 0\\ 0 & 0 & -\beta_A S_A & -\beta_A S_A & 0 & 0\\ 0 & 0 & -\beta_C U_C^V\,\epsilon & -\beta_C U_C^V\,\epsilon & 0 & 0\\ 0 & 0 & -\beta_A U_A^V\,\epsilon & -\beta_A U_A^V\,\epsilon & 0 & 0\\ 0 & 0 & 0 & 0 & 0 & 0\\ 0 & 0 & 0 & 0 & 0 & 0\\ -\delta-\mu-\psi & 0 & \beta_C S_C+\beta_C U_C^V\epsilon & \beta_C S_C+\beta_C U_C^V\epsilon & 0 & 0\\ \psi & -\delta-\mu & \beta_A S_A+\beta_A U_A^V\,\epsilon & \beta_A S_A+\beta_A U_A^V\epsilon & 0 & 0\\ \delta & 0 & -\gamma-d-\mu-\psi & 0 & 0 & 0\\ 0 & \delta & \psi & -\gamma-d-\mu & 0 & 0\\ 0 & 0 & \gamma & 0 & -\mu-\psi & 0\\ 0 & 0 & 0 & \gamma & \psi & -\mu \end{pmatrix}.$$

Let λ_i, $i = 1, 2, \ldots 12$, be eigenvalues of the matrix J_0. Then $\lambda_1 = -\mu$, $\lambda_2 = -(\mu + \xi_A)$, $\lambda_3 = -(\mu + \psi)$, $\lambda_4 = -(\mu + \eta_M)$, $\lambda_5 = -(\mu + \eta_A)$, $\lambda_6 = -(\mu + \eta_A)$, $\lambda_7 = -(\mu + \eta_U + \psi)$,

$\lambda_8 = -(\mu + \xi_M + \xi_U + \psi)$, $\lambda_9 = -(\gamma + d + \mu + \psi)$, $\lambda_{10} = -(\delta + \mu + \psi)$,

$$\lambda_{11} = -\frac{1}{2}\left(d+\delta+2\mu+\gamma+\sqrt{(\gamma+d+\delta+2\mu)^2-4(1-R_v)(\delta+\mu)(\gamma+d+\mu)}\right),$$

$$\lambda_{12} = -\frac{1}{2}\left(d+\delta+2\mu+\gamma-\sqrt{(\gamma+d+\delta+2\mu)^2-4(1-R_v)(\delta+\mu)(\gamma+d+\mu)}\right).$$ All eigenvalues are negative except λ_{12}, which is also negative for $R_v < 1$. Thus, we can conclude that the disease-free equilibrium point is locally asymptotically stable for $R_v < 1$.

In the epidemiological sense, the locally asymptotically stability of the disease-free equilibrium for $R_v < 1$ implies that the measles dynamics initiated with a small number of infections introduced in the community approaches to the measles-free state over time when the vaccinated reproduction number remains less than one. In other words, the vaccinated reproduction number being less than unity assures that the disease outbreak will die out when a small population perturbation occurs with the introduction of a small number of infections, which is usually the case at the beginning of infection. Such a condition allows us to design a vaccination policy that assures $R_v < 1$, thereby avoiding the outbreak. However, local stability does not ensure outbreak control under all conditions or if the system is perturbed significantly.

3.3.2. Global stability of the disease-free equilibrium E^0

In this section, we show that $R_v < 1$ also asserts the global stability of the disease-free equilibrium E^0 as stated in the following theorem.

Theorem 3.2. *The disease-free equilibrium E^0 is globally stable when $R_v < 1$.*

Here, we determine the global stability of E^0 using the results presented in a previous study (Castillo-Chávez et al., 2002). First, system (1–12) is written as $dX/dt = F(X, Y)$, $dY/dt = G(X, Y)$, with $G(X, 0) = 0$, where $X \in R^8$ and $Y \in R^4$ represent the uninfected and infected compartments, respectively. Then satisfying the following two conditions implies the global asymptotically stability of the system around disease-free equilibrium point $E^0 = (X^*, 0)$:

1. For $dX/dt = F(X, 0)$, X^* is globally stable, (where $X^* \in R^8$ at disease free state) and
2. $\hat{G}(X,Y) = BY - G(X,Y) \geq 0$, for $(X, Y) \in R^{12}$, where B is the Jacobian of the infected system at the disease-free equilibrium E^0.

Clearly, the system

$$\frac{dX}{dt} = \begin{pmatrix} \Lambda - S_C(\mu + \xi_M + \xi_U + \psi) \\ S_C\,\psi - \mu S_A \\ S_C\xi_U - U_C^V(\mu + \eta_U + \psi) \\ U_C^V\psi - U_A^V(\mu + \eta_A) \\ \xi_A S_A - V_A(\mu + \eta_A), \\ S_C\xi_M - M_C^V(\mu + \eta_M) \\ M_C^V\eta_M - I_{mC}(\mu + \psi) + U_C^V\eta_U \\ (U_A^V + V_A)\eta_A - \mu I_{mA} + I_{mC}\,\psi \end{pmatrix}$$

is globally asymptotically stable at X^*. The matrix of the infected compartments is given as:

$$G = \begin{pmatrix} (I_C + I_A)\beta_C S_C + (I_C + I_A)\beta_C U_C^V\epsilon - (\delta + \mu + \psi)E_C \\ (I_C + I_A)\beta_A S_A + (I_C + I_A)\beta_A U_A^V\epsilon + E_C\psi - E_A(\delta + \mu) \\ E_C\delta - I_C(\gamma + d + \mu + \psi) \\ E_A\delta + I_C\psi - I_A(\gamma + d + \mu) \end{pmatrix}.$$

The Jacobian of the matrix G at the disease-free equilibrium is $B =$

$$\begin{pmatrix} -\delta - \mu - \psi & 0 & \beta_C(S_C)^0 + \beta_C\left(U_C^V\right)^0\epsilon & \beta_C(S_C)^0 + \beta_C\left(U_C^V\right)^0\epsilon \\ \psi & -\delta - \mu & \beta_A(S_A)^0 + \beta_A\left(U_A^V\right)^0\epsilon & \beta_A(S_A)^0 + \beta_A\left(U_A^V\right)^0\epsilon \\ \delta & 0 & -\gamma - d - \mu - \psi & 0 \\ 0 & \delta & \psi & -\gamma - d - \mu \end{pmatrix}.$$

$$Y = \begin{pmatrix} E_C \\ E_A \\ I_C \\ I_A \end{pmatrix},$$

$$BY = \begin{pmatrix} -E_C(\delta + \mu + \psi) + (I_C + I_A)\beta_C(S_C)^0 + (I_C + I_A)\beta_C\left(U_C^V\right)^0\epsilon \\ -E_A(\delta + \mu) + (I_C + I_A)\beta_A(S_A)^0 + (I_C + I_A)\beta_A\left(U_A^V\right)^0\epsilon + E_C\psi \\ E_C\delta - I_C(\gamma + d + \mu + \psi) \\ -I_A(\gamma + d + \mu) + E_A\delta + I_C\psi \end{pmatrix},$$

where Y is a (4×1) matrix with elements (E_C, E_A, I_C, I_A). Then $BY - G$ or $\hat{G} =$

$$\begin{pmatrix} (I_C + I_A)\beta_C\left(\left(\frac{\Lambda}{\mu + \xi_M + \xi_U + \psi} - S_C\right) + \epsilon\left(\frac{\Lambda\xi_U}{Z(\mu + \xi_M + \xi_U + \psi)} - U_C^V\right)\right) \\ (I_C + I_A)\beta_A\left(\epsilon\left(\frac{\Lambda\psi\xi_U}{Z(\eta_A + \mu)(\mu + \xi_M + \xi_U + \psi)} - U_A^V\right) + \left(\frac{\Lambda\psi}{(\mu + \xi_A)(\mu + \xi_M + \xi_U + \psi)} - S_A\right)\right) \\ 0 \\ 0 \end{pmatrix}.$$

From the system of equations 1–12, we ultimately obtain

$$S_C \leq \frac{\Lambda}{\mu+\xi_M+\xi_U+\psi}, S_A \leq \frac{\Lambda\psi}{(\mu+\xi_A)(\mu+\xi_M+\xi_U+\psi)}, U_C^V \leq \frac{\Lambda\xi_U}{Z(\mu+\xi_M+\xi_U+\psi)}, \text{and } U_A^V \leq \frac{\Lambda\psi\xi_U}{Z(\eta_A+\mu)(\mu+\xi_M+\xi_U+\psi)}.$$

Clearly $(BY - G)$ is the non-negative matrix for $R_v < 1$, so the disease free equilibrium point is globally asymptotically stable when $R_v < 1$.

Epidemiologically, our theorem establishing the global stability of the disease-free equilibrium implies that the disease can't establish sustained transmission within the population for any, even significantly large, initial number of infections as long as $R_v < 1$. The global stability of the disease-free equilibrium point of our model helps to maintain and implement preventive strategies such as vaccination programs for disease control.

3.4. Endemic equilibrium

Obtaining the endemic point in the infectious disease modeling is crucial to understanding the long-term disease dynamics. For many situations with imperfect vaccination programs, which is likely the current condition in Nepal, the endemic equilibrium provides the epidemic's severity. The epidemic level, at least, informs important policy guidelines for disease control if not eradicated.

Suppose $E^* = \left(S_C^*, S_A^*, (U_C^V)^*, (U_A^V)^*, V_A^*, (M_C^V)^*, E_C^*, E_A^*, I_C^*, I_A^*, I_{mC}^*, I_{mA}^*\right)$ be an endemic equilibrium of the system. Let, $I^* = I_C^* + I_A^*$. Then solving system (1–12), we get

$$\begin{aligned}
S_C^* &= \frac{\Lambda}{\beta_C I^* + \mu + \xi_M + \xi_U + \psi},\\
S_A^* &= \frac{\Lambda\psi}{(\beta_A I^* + \mu + \xi_A)(\beta_C Ia^* + \mu + \xi_M + \xi_U + \psi)},\\
\left(U_C^V\right)^* &= \frac{\Lambda\xi_U}{(\beta_C I^* + \mu + \xi_M + \xi_U + \psi)(\beta_C I^*\epsilon + Z)},\\
\left(U_A^V\right)^* &= \frac{\Lambda\psi\xi_U}{(\eta_A + \beta_A I^*\epsilon + \mu)(\beta_C I^* + \mu + \xi_M + \xi_U + \psi)(\beta_C I^*\epsilon + Z)},\\
V_A^* &= \frac{\Lambda\psi\xi_A}{(\eta_A + \mu)(\beta_A I^* + \mu + \xi_A)(\beta_C I^* + \mu + \xi_M + \xi_U + \psi)},\\
\left(M_C^V\right)^* &= \frac{\Lambda\xi_M}{(\mu + \eta_M)(\beta_C I^* + \mu + \xi_M + \xi_U + \psi)},\\
E_C^* &= \frac{\beta_C I^* \Lambda(\beta_C I^*\epsilon + \epsilon\,\xi_U + Z)}{(\delta + \mu + \psi)(\beta_C I^* + \mu + \xi_M + \xi_U + \psi)(\beta_C I^*\epsilon + Z)},\\
I_C^* &= \frac{\beta_C \delta I^* \Lambda(\beta_C I^*\epsilon + \epsilon\,\xi_U + Z)}{(\delta + \mu + \psi)(\gamma + d + \mu + \psi)(\beta_C I^* + \mu + \xi_M + \xi_U + \psi)(\beta_C I^*\epsilon + Z)}.
\end{aligned}$$

Here, $E_A^*, I_A^*, I_{mC}^*, I_{mA}^*$ are positive when $R_v > 1$ (see supplementary file). After manipulating the equations of the system at diseased equilibrium we obtained the equation given as:

$$(A_4(I^*)^4 + A_3(I^*)^3 + A_2(I^*)^2 + A_1 I^* + A_0)I^* = 0, \tag{13}$$

where,

$$\begin{aligned}
A_4 &= \beta_C^2\beta_A^2\epsilon^2(\delta+\mu)(\gamma+d+\mu),\\
A_0 &= (1-R_v)(\delta+\mu)(\eta_A+\mu)(\xi_A+\mu)(\gamma+d+\mu)(\mu+\eta_U+\psi)(\mu+\xi_M+\xi_U+\psi),
\end{aligned}$$

and A_1, A_2, A_3 are provided in supplementary file. Note that $I^* = 0$ corresponds to the disease-free equilibrium E^0. Since $A_0 < 0$ when $R_v > 1$ and $A_4 > 0$, then by Vieta's Theorem, there exists at least one positive I^* and the system has at least one endemic equilibrium when $R_v > 1$.

We can compute the magnitude of endemic equilibrium by solving Eq. (13). We were unable to establish the stability of the endemic equilibrium analytically due to the complexity brought by the higher-order equations with nonlinearity. However, we performed numerical analysis for the stability of the endemic equilibrium and presented results as a bifurcation diagram

with the existence and stability of the endemic equilibrium for $R_v > 1$ (Fig. 3), for which the disease-free equilibrium is unstable.

4. Numerical simulations

4.1. Data fitting, model validation, and parameter estimation

Since measles cases were found only in ten districts of Nepal (Fig. 1), we considered the population corresponding to only these ten districts with a total of $N(0) = 6,564,070$ (N. S. Office, 2021). Moreover, as the cases appeared only in a few villages of these ten districts, the whole population is less likely to be in the contact network. Therefore, we assume α is a portion of the total population, so only $\alpha N(0)$ is in the measles transmission contact network. In Nepal, the children population aged up to 14 years is 27.4% (Statista, 2023), so we assumed 29% of the total population aged up to 15 years and took $N_C(0) = 0.29\alpha N(0)$ and $N_A(0) = 0.71\alpha N(0)$.

The vaccinated population in Nepal is about 87–93% (WHO, 2023c), and assuming children are more vaccinated than adults, we took 91% of children and 89% of adults were vaccinated. Thus, we took 9% and 11% of unvaccinated children and adults as respective susceptibles, i.e., $S_C(0) = 0.09\alpha N_C(0)$ and $S_A(0) = 0.11\alpha N_A(0)$. Since there was no adequately monitored vaccination or catch-up program for adult vaccination in Nepal, we took $M_C^V(0) = 50,\ V_A = 0$. Since vaccine effectiveness for measles is 77–86% (Ichimura et al., 2022; Kumar et al., 2023; Lochlainn et al., 2019), we took 89% as the immune population, giving $I_{mA}(0) = 0.79\alpha N_A(0)$ and $I_{mC}(0) = 0.81\alpha N_C(0)$. The remaining populations are taken as $U_C^V(0)$ and $U_A^V(0)$. Following the magnitude of data, we assume that the outbreak begins with a small number of exposed and infected individuals and took $E_C(0) = 5$, $E_A(0) = 3$, $I_C(0) = 2$, $I_A(0) = 1$.

For this study, individuals under 15 were categorized as children, giving the maturation rate of $\psi = 1/(15 \times 52) = 0.0013$ per week. Since the average lifespan for Nepal in 2023 is approximately 72 years (Macrotrends), we took the natural death rate as $1/(72 \times 52)$ per week. During the period of data collected, no immunization program was in place for adults, so we took both the rate of adult vaccination (ξ_A) and the rate of being immune through adult vaccination (η_A) as zero. We also assume the rate of adults being immune through un-monitored vaccination (η_A) to be zero.

We considered the incubation period for measles to be 10 days (range: 10–14 days) (WHO, 2023a), implying $\delta = 0.7$ per week. Considering the recovery period from the disease is around 15 days (range: 7–23 days) (WHO-Nepal, 2023b), we obtain $\gamma = 1/2$ per week. Using the Case Fatality Rate (CFR) of 0.14% in Nepal (Dall, 2023; WHO-Nepal, 2023a) in the disease-induced death rate formula $d = \frac{-ln(1-0.14/100)}{T}$ given in the previous study (Pantha, Giri, Joshi, & Vaidya, 2021) with $T = 15$ weeks, we obtain $d = 9.3399 \times 10^{-5}$ per week.

In line with WHO guidelines, children receive their first vaccine dose at 9 months of age and the second dose at 15 months (MoHP, 2024), with a six-month interval between two doses. Accounting for an average vaccine effectiveness of 80 % (Min-Shi et al., 2009; WHO-Measles, 2019), we adopted $\epsilon = 1 - 0.8 = 0.2$. Since the outbreaks usually remain for a short term of 15 weeks only, as revealed in the data, we can assume that the birth and the death balance each other, i.e., $\Lambda = \mu \times N$.

We estimate the parameters β_C, β_A, ξ_U, η_U, η_M, and α by fitting the model with the measles case data from Nepal. From the model, weekly new infections at time t are given by $h(t) = \theta\delta E(t)$, which we obtain using the numerical solutions of system (1-

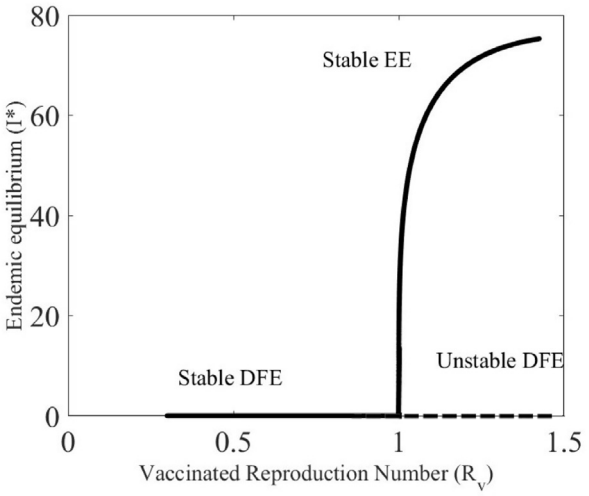

Fig. 3. Forward bifurcation at $R_v = 1$. The disease free equilibrium is stable for $R_v < 1$. The disease free is unstable and endemic equilibrium is stable for $R_v > 1$.

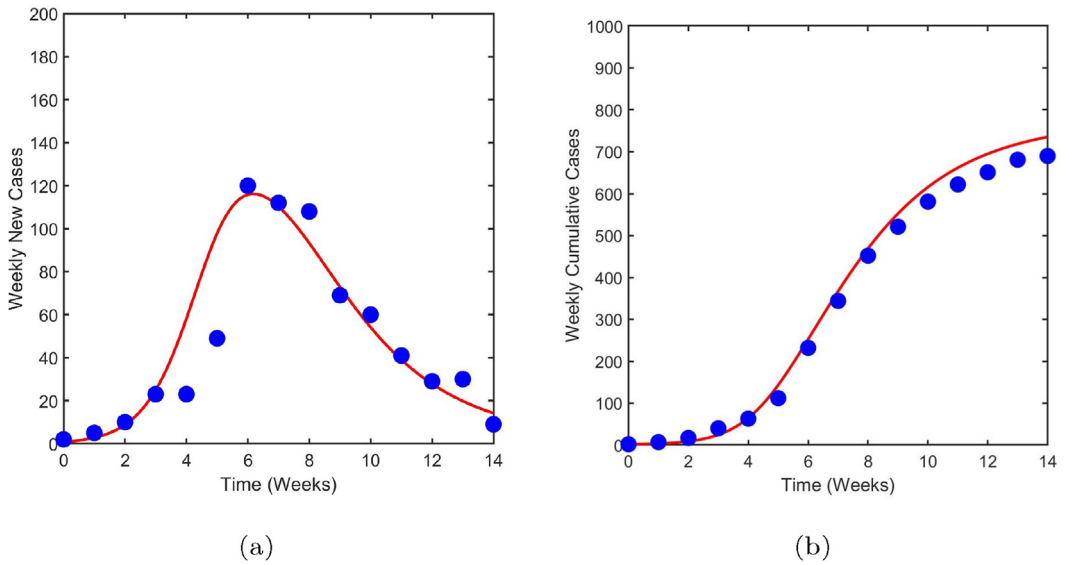

Fig. 4. Data fitting and model validation. (a) The recorded weekly cases of measles in Nepal (filled circle) along with the best fit of the model (line). (b) The cumulative recorded measles cases in Nepal (filled circle) along with the model prediction of the cumulative cases (line).

12). Here, θ represents the portion of the infection recorded. Then, we estimate the parameters with the help of the nonlinear regression method (Motulasky & Arthur, 2003) that minimizes the following sum of the square residuals:

$$\sum_{k=1}^{15} (h_k - \bar{h}_k)^2,$$

where h_k denotes the model predicted weekly new infection and $\bar{h}_k$ denotes weekly new infection data. All the computations are carried out in MATLAB (The Math Works. Inc.) using its various routines, including "ode45" (ODE solver) and "fmincon" (minimizer).

Our model can fit the data of weekly incidence cases in Nepal well (Fig. 4a). In addition, we also show that the model prediction of the cumulative cases agrees well with the cumulative data (Fig. 4b), thereby validating our model. The values of state variables and parameters are given in Table 2 and Table 3, respectively. From our estimation, the transmission rate in children ($\beta_C = 0.00188$) is higher than in adults ($\beta_A = 1.00 \times 10^{-5}$). Despite the low transmission rate among adults, it may still be sufficient to spread the disease and cause obstacles to achieving the mission of measles eradication. Similarly, we obtained the monitored vaccination rate ($\xi_M = 4.777 \times 10^{-6}$) is less than the un-monitored vaccination rate ($\xi_U = 0.0087$), and the rate of being immune from monitored vaccination ($\eta_M = 0.0167$) is higher than the un-monitored vaccination ($\eta_U = 3 \times 10^{-6}$). Our estimates indicate that about 15% of the measles cases were recorded in Nepal (*i.e.*, $\theta = 0.15$) (Table 3).

4.2. Parameter sensitivity analysis

4.2.1. Sensitivity of R_v

We quantify the local sensitivity of R_v to each of the parameters β_C, β_A, ψ, γ, d, δ, ϵ, μ, η_A, η_U, η_M, ξ_M, ξ_U, and ξ_A. For this, we obtained the sensitivity index, S_x, for each parameter x using the relationship:

$$S_x = \left(\frac{x}{R_v}\right)\left(\frac{\partial R_v}{\partial x}\right).$$

Based on the sensitivity index S_x, we found that the parameter γ affects R_v the most compared to the other parameters. The second parameter affecting R_v is β_C, followed by the parameters ϵ, ψ, μ, ξ_U, and β_A, while the effects of d, δ, η_A, η_M, ξ_A, η_M and ξ_M to R_v are negligible (Fig. 5a).

We also performed the global sensitivity analysis by using the Latin Hypercube Sampling (LHS) technique (Simeone, Hogue, Ray, & Kirschner, 2008) with 1000 samples of parameter sets from a wider parameter range of ±25% of the base value of each parameter. We compute the partial rank correlation coefficients (PRCC) to identify the most influential parameter to R_v. We observed that the parameters γ, β_C, ϵ, and ψ are the most sensitive parameters for R_v, which are followed

Table 2
State variables.

State Variables	Values	State Variables	Values
$M_C^V(0)$	50	$V_A(0)$	0
$E_C(0)$	5	$E_A(0)$	3
$I_C(0)$	2	$I_A(0)$	1
$S_C(0)$	2142	$S_A(0)$	6408
$U_C^V(0)$	2382	$U_A^V(0)$	5703
$I_{mC}(0)$	19,271	$I_{mA}(0)$	46,145
$N_C(0)$	23,795	$N_A(0)$	58,256

Table 3
Model parameters.

Symbols of Parameters	Values	Source
ξ_U, ξ_M	0.087, 4.77×10^{-5}	Data fitting
β_C, β_A	0.00188, 1.00×10^{-5}	Data fitting
μ	$1/(72 \times 52)$	Calculated
γ	1/2	WHO-Nepal (2023b)
ψ	$1/(15 \times 52)$	Calculated
ϵ	0.2	[46, 47]
η_A	0	Assumed
η_U, η_M	3×10^{-6}, 0.167	Data fitting
δ	0.7	WHO-Nepal (2023b)
θ	0.15	Data fitting
d	9.3399×10^{-05}	Calculated
ξ_A	0	Assumed
α	0.01253	Data fitting

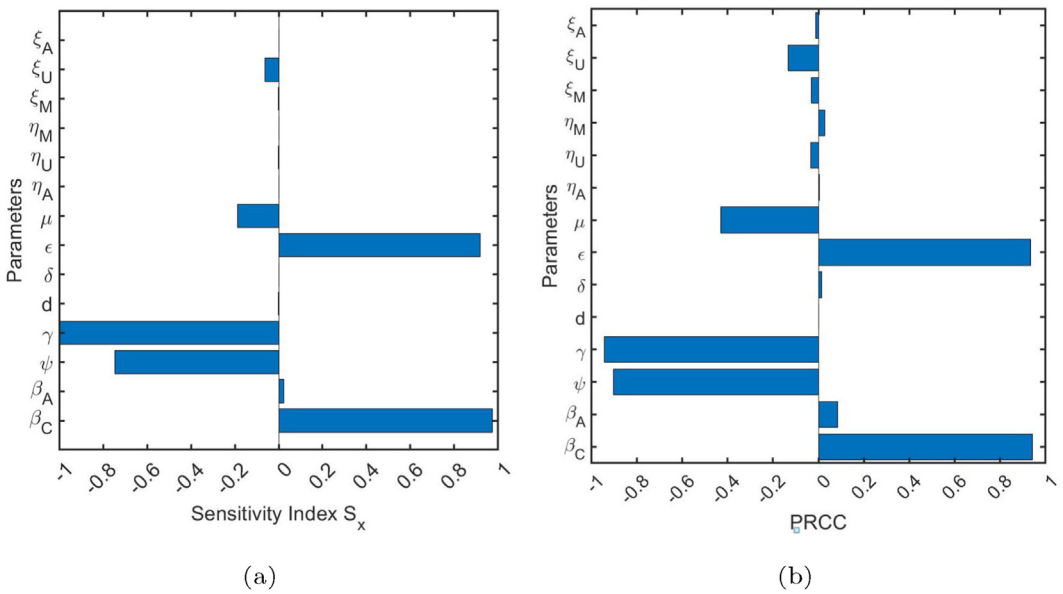

Fig. 5. (a) Local sensitivity of parameters to R_v. The sensitivity index, S_x, showing the level of change in R_v with respect to the parameters. Note that the sensitivity index S_x of d, δ, η_A, η_U, η_M, ξ_A and ξ_M are negligible and difficult to visualize in the figure. **(b) Global sensitivity of R_v.** Partial Rank Correlation Coefficients for R_v from LHS method.

by μ, ξ_U, and β_A, and the rest of the parameters are less effective (Fig. 5b). Both local and global analyses show that R_v is mostly influenced by the parameters γ, β_C, and ϵ.

4.2.2. Sensitivity of measles dynamics

We also used the Latin Hypercube Sampling (Simeone, Hogue, Ray, & Kirschner, 2008) method to explore the global sensitivity of the measles dynamics represented by the peak infection and the time to peak in adults, children, and combined. The computed partial rank correlation coefficient corresponding to each parameter is presented in Fig. 6. Our analysis shows

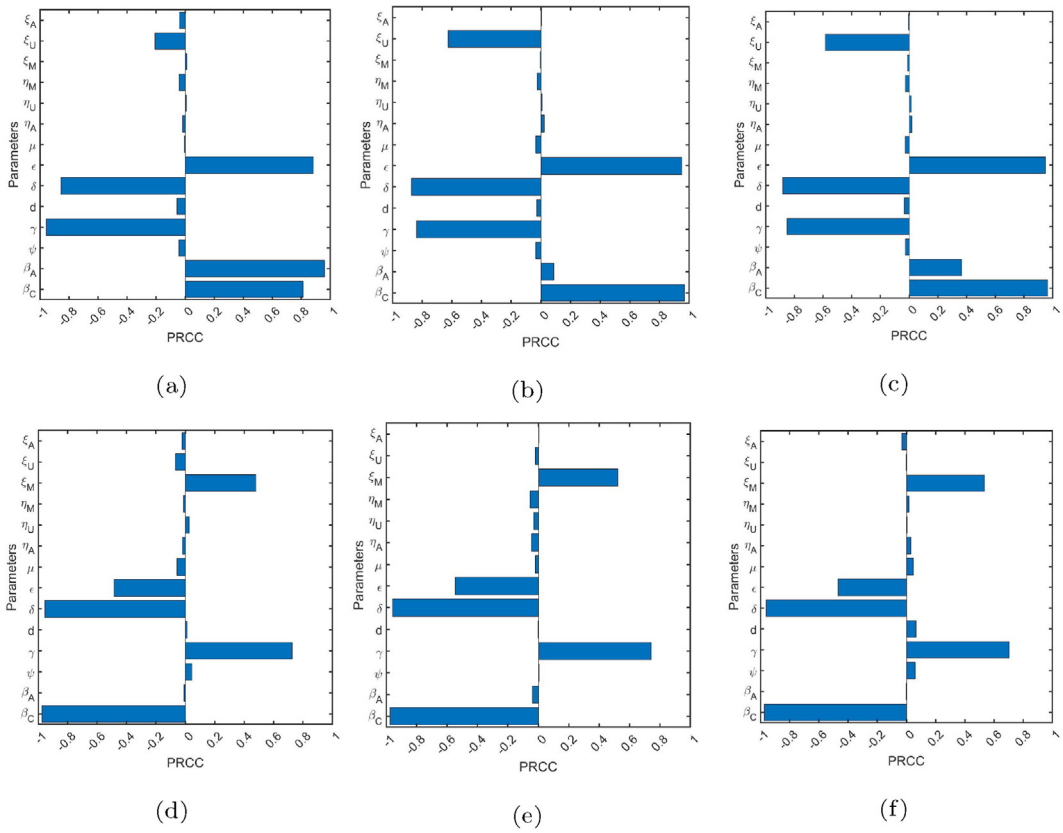

Fig. 6. Sensitivity of measles dynamics. Global sensitivity of the parameters to peak value and time to peak infection for adult I_A (a, d), children I_C (b, e), and combined child and adult (c, f). The partial rank correlation coefficients for sensitivity are based on 1000 Latin Hypercube Sample sets of parameters.

that the peak value of the infected class I_A is highly influenced by γ, β_A, ϵ, and δ followed by β_C and then by ξ_U while the remaining parameters are less effective (Fig. 6a). Also, the peak value of the infected class I_C is highly influenced by β_C, ϵ, δ, and γ, followed by ξ_U and other parameters are less effective (Fig. 6b). Similarly, the peak value of the infected class of children and adults combined is influenced by the parameters β_C, ϵ, δ, γ, followed by ξ_U. In contrast, the remaining parameters are less effective (Fig. 6c).

The time to peak infection is mostly affected by the parameters β_C, δ, and γ, followed by ϵ and ξ_M. The rest of the parameters in I_A and I_C less influences it. Similarly, the time to peak for combined infection is mainly affected by δ, β_C, γ, and ϵ, followed by ξ_M, while the remaining parameters are less effective (Fig. 6f).

4.3. Impact of the contact network on infection

While we estimated the base contact network in the data context, the contact network may change depending on the situation. Therefore, we now explore the effects of the contact network on the total number of infections and its peak value for each infected class. An increase in children's contact network by 5, 10, and 15 times the base case results in the rise of peak infection of children by 8, 16, and 21 times, respectively, and an increase in the total children infection by 4, 7, and 8 times, respectively (Fig. 7a). Similarly, the same increment level in the adult contact network results in the increment of the total infection by 28, 85, and 133 times and the peak infection by 28, 92, and 166 times, respectively (Fig. 7b). An increment in the contact network of all populations by 5, 10, and 15 times results in an increment of approximately 8, 17, and 23 times in the peak infection and 7, 16, and 23 times in the total infection, respectively (Fig. 7c).

4.4. Impact of monitored vaccine program

4.4.1. On disease increase-decrease trend

Here, we examine the profound role of vaccine coverage in the increase-decrease trend of the disease, i.e., reducing the effective reproduction number (R_e) below one. We evaluate the effect of both timeliness and extension of vaccination

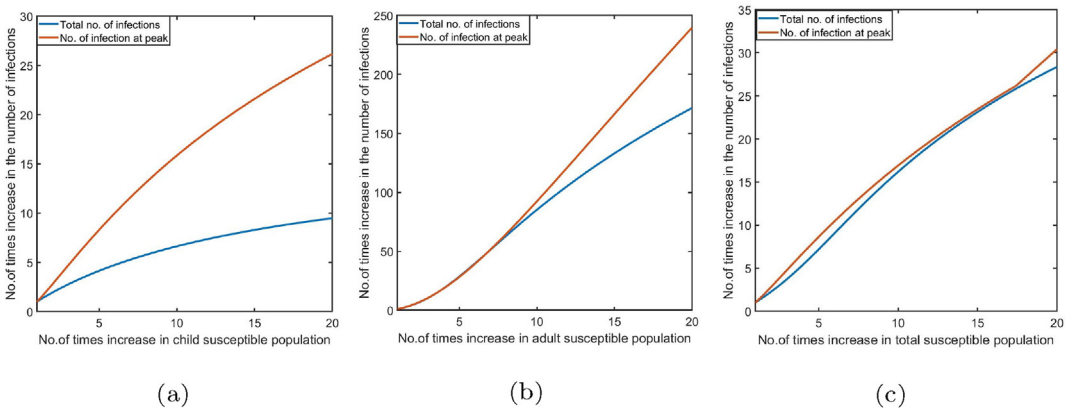

Fig. 7. Effects of the contact network size. The total number of infections and peak infection on the variation of the contact network of (a) children, (b) adults, and (c) total (children and adults).

coverage in achieving the goal of $R_e < 1$ (decreasing trend). Our findings show that complete vaccine coverage within the first two weeks of outbreaks yields remarkable outcomes in lowering the effective reproduction number. Achieving a vaccination coverage of over 90% among children within two weeks decreases the effective reproduction number to below 1 in just two weeks. In contrast, when vaccine coverage is limited to only 20%, this critical threshold is reached only after six weeks (Fig. 8a).

Our model predicts that a vaccination campaign focused only on adults may not be sufficient to reduce the effective reproduction number to below one within a reasonable time frame. As depicted in Fig. 8b, the complete vaccine coverage of adults within two weeks slightly lowers the effective reproduction number in about seven weeks. The vaccination distributed among the combined population is less effective than the vaccination entirely given to children. In this case, the threshold can be lowered to below one in one week by 90% of vaccine coverage within three weeks, while it takes six weeks for 30% of coverage within two weeks (Fig. 8c).

4.4.2. On the reduction of disease burden

We also explore the impact of vaccine coverage over a specific period on reducing measles cases and the maximum weekly cases. Our modeling reveals a significant variation in the effects of vaccine coverage across distinct age groups (Fig. 9). 20% of children vaccination within two weeks can reduce about 85% of the total measles cases and 85% of the maximum weekly cases, while 90% of children vaccination within six weeks can reduce more than 90% of the total measles cases and more than 90% of the maximum weekly cases (Fig. 9a and b). In contrast, 20% of adult vaccinations within two weeks can reduce only 10% of the total cases and only 5% of the maximum weekly cases. Even 90% of the adult vaccinations within six weeks can reduce only 12% of the total cases and only 7% of the maximum weekly cases (Fig. 9c and d).

90% of combined adult-child vaccination within two weeks reduces about 80% of the total measles cases and 80% of the maximum weekly cases (Fig. 9e and f). These results highlight that the effectiveness of vaccination in diminishing measles

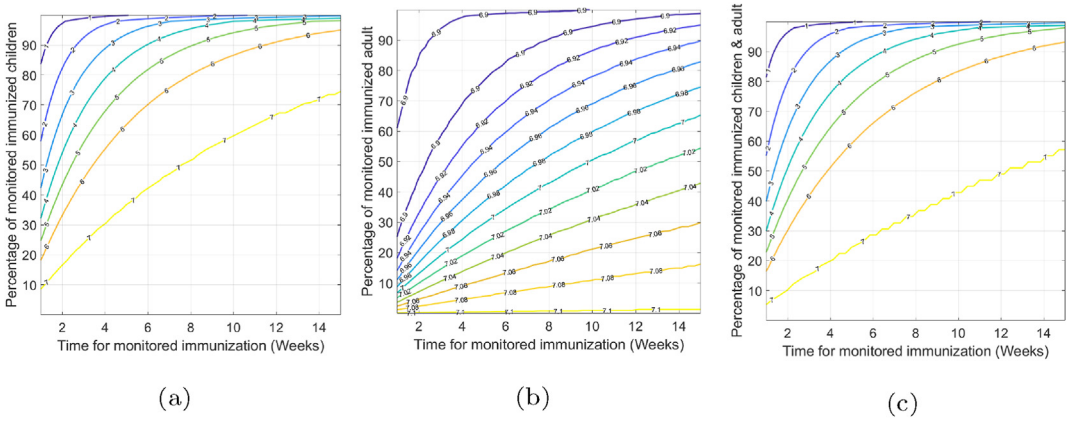

Fig. 8. Time for R_e<1. Time (in weeks) for the effective reproduction number to be less than one when (a) only children are immunized, (b) only adults are immunized, and (c) children and adults are immunized.

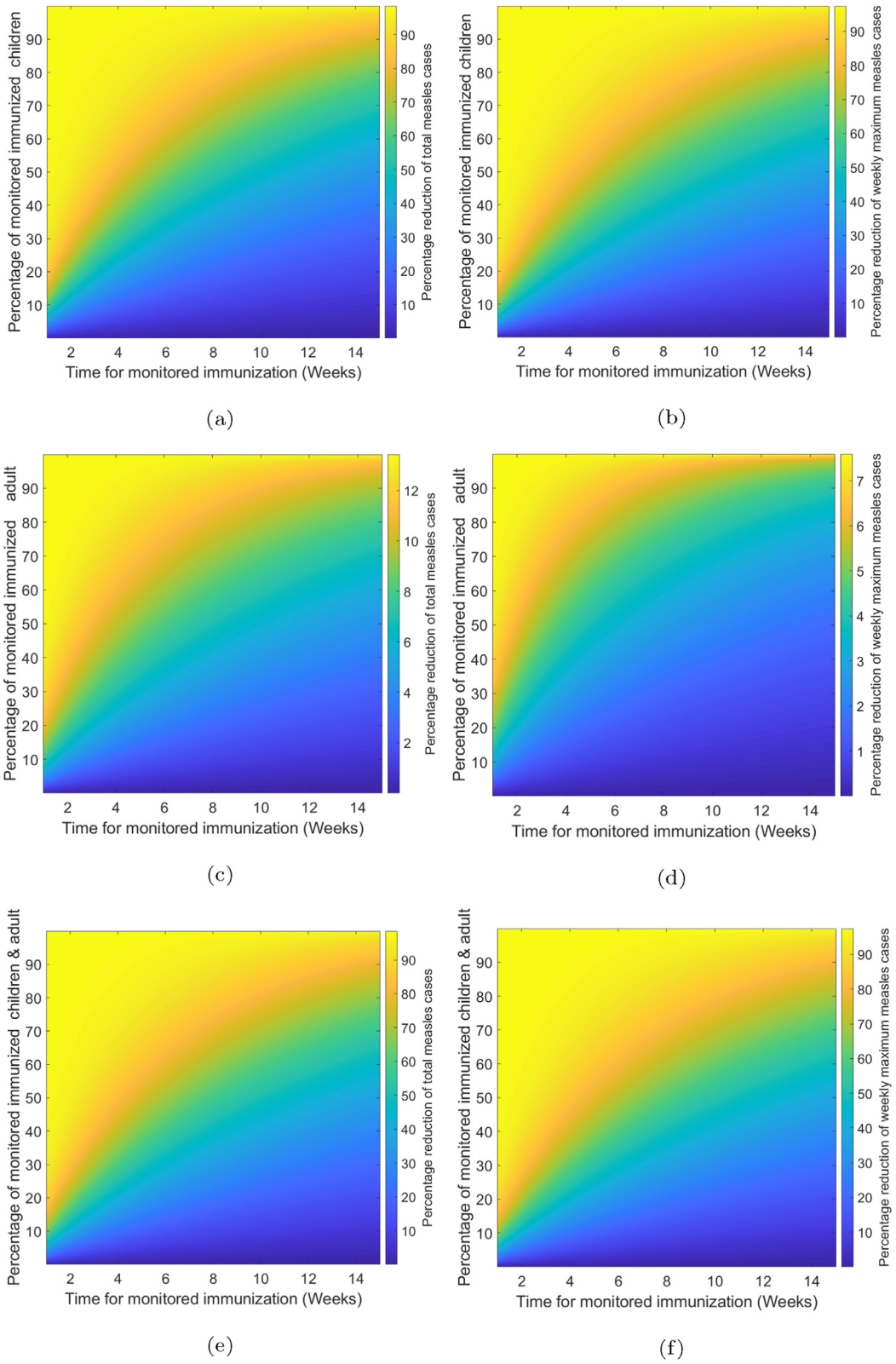

Fig. 9. Effects of monitored vaccination. Impact of the coverage of monitored children vaccination on the percentage reduction of (a) the total measles cases and (b) weekly maximum new cases of measles, adult vaccination on the percentage reduction of (c) the total measles cases and (d) weekly maximum new cases of measles, the children and adult vaccination on the percentage reduction of (e) the total measles cases and (f) weekly maximum new cases of measles.

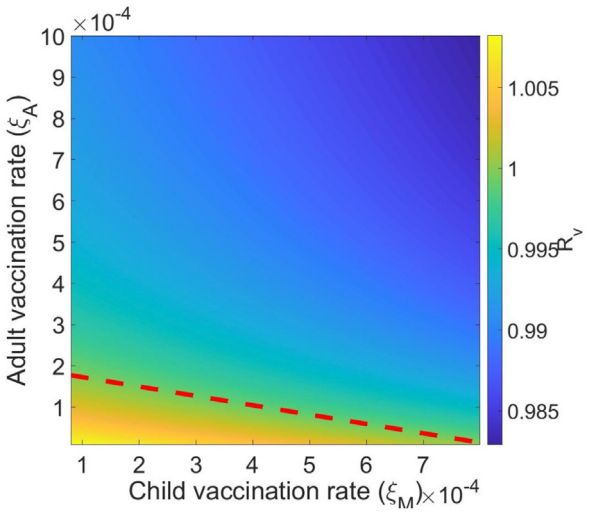

Fig. 10. Effects of vaccination on R_v. Value of R_v for combinations of children and adults vaccination rates (ξ_M-ξ_A parameter space). The dashed red line corresponds to $R_v = 1$.

prevalence is notably more pronounced in vaccination programs focused on children (Fig. 9a) than adults (Fig. 9c). However, it is worth noting that even though the adult vaccination may reduce the burden negligibly compared to childhood vaccination, it still plays a vital role in controlling the disease, especially for eradication, since adults may act as a potential reservoir source for persistent disease transmission.

4.5. Infections in adults: implications to disease eradication

As found above, vaccination focused on adults only has the negligible benefit of reducing the disease burden compared to vaccination focused on children. However, persistent infection in adults may pose an obstacle to measles eradication. Therefore, we further performed a deeper analysis to explore whether a realistic adult infection-related parameter range exists that may cause an obstacle to eradication. To examine this, we identified the region corresponding to the disease eradication ($R_v < 1$) and disease persistence ($R_v > 1$) in the ξ_M-ξ_A parameter space of children and adults vaccination rates (Fig. 10).

As illustrated in Fig. 10, with the parameter range $3 \leq \xi_M \leq 17(\times 10^{-5})$ and $0 \leq \xi_A \leq 10(\times 10^{-4})$, we observe that there exists a realistic parameter range (space below $R_v = 1$ curve in Fig. 10) for which $R_v > 1$. This indicates that unless the child vaccination rate is sufficiently large, the value of R_v may remain above one due to some persistent infection in adults. In this case, introducing adult vaccination on top of the child vaccination can reduce R_v below one. Therefore, in the situation when children-focused vaccination is not sufficiently large enough, which is likely the case in developing countries like Nepal, persistent infection in adults can be a major hurdle for disease eradication, and considering adult-focused vaccination along with children's vaccination becomes critical for global disease eradication.

5. Discussion

In recent years, measles outbreaks have occurred frequently in many places of the globe. The threat of measles is growing due to the expansion of immunity gaps, COVID-19's disruption of routine immunization, and the lack of planned global vaccination campaigns. The reduction of vaccination is also attributed to various factors, including societal and educational impacts and religious barriers. In Nepal, the decline in vaccination coverage corresponds to the patterns of measles epidemics. While a higher proportion of cases are observed in young infants and older children, a small number of cases have frequently been observed in Nepalese adults (WHO, 2023d), implying that the unvaccinated adults may serve as a virus reservoir to cause obstacles to WHO's eradication goal. The model developed in this study with both children and adult groups is essential to identify the ideal monitored vaccination strategy for both adults and children to ensure the global eradication of measles.

Using our model validated by the measles case data of different regions of Nepal from November 24, 2022, to March 10, 2023 (WHO-Nepal, 2023a), we estimated the measles-vaccinated reproduction number in Nepal to be $R_v = 11.677$. The value of R_v is much higher than one, indicating that significant efforts need to be put into the vaccination program in Nepal to meet WHO's global eradication goal. Most notably, our model predicts a critical adult vaccination level required in combination with a partially successful children's vaccination program to bring R_v less than one. Therefore, our study underscores the need for combined adult and children vaccination for measles eradication, in contrast to the often ignored adult group in vaccination programs.

We explored the effect of the contact network size on measles epidemics. We found that increasing contact networks ultimately increases the total and weekly measles cases in children and adults. Interestingly, the increase in measles burden is more pronounced due to the rise of contact networks among adults than children, mainly when the increased level is more than ten times the base case. This result further highlights the importance of adult vaccination, which lowers the adult susceptible population, thereby reducing the total infection and weekly infection.

We also examined the impact of vaccine coverage on disease trends (Fig. 8) and the disease burden (Fig. 9). Our model helps identify a reasonable level of child-adult vaccine coverage to ensure the decreasing trend of measles (i.e., $R_e < 1$). For example, 90% in three weeks or 30% in two weeks of vaccine coverage can bring R_e less than one in one day or six days, respectively. Similarly, our model allows us to properly evaluate the vaccination program for reducing the disease burden. For example, an 80% reduction in the total measles cases and an 80% reduction in the maximum weekly cases can be achieved by covering 90% adult and child population within two weeks of vaccination. Our results show that the vaccine focused entirely on children can reduce the disease burden more than that distributed among both children and adults, highlighting the significance of prioritizing childhood vaccine coverage as a primary strategy for reducing disease burden. However, as discussed above, adult vaccination should not be overlooked as it may have a critical role in disease eradication. Our result is consistent with the previous studies (Dipo & Dinda, 2019; Garba et al., 2017; Jaharuddin, 2020; Lessler et al., 2016; Pokharel et al., 2022).

We acknowledge some limitations of our study. The parameter estimations were based on the limited data of weekly incidence cases. The lack of granular data and information could have hindered the achievement of more accurate outcomes. Although we successfully derived the closed form of the distinct endemic equilibrium, we were unable to complete a thorough analysis of this equilibrium due to model complexities. For example, we couldn't achieve the stability condition of endemic equilibrium, while we only explored the stability of endemic equilibrium through numerical methods. We have ignored the potential effects of spatial heterogeneity on disease transmission and assumed a homogenous mixed population. Spatial heterogeneity may play a role in disease transmission, especially in the spread of measles in some specific districts of Nepal. Further study on the cost-effectiveness analysis based on the country's financial status would benefit the optimal policy design to achieve the measles eradication goal.

In summary, we developed a novel model of measles transmission in the context of Nepal, incorporating the two different age groups, children (15 and under) and adults (above 15). Our model demonstrates that the adult group is a potential reservoir of measles, causing obstacles to eradicating the disease. Our results suggest that implementing the adult vaccines along with the children's vaccine is critical for achieving WHO's global measles eradication goal. A well-planned adult-child combination of monitored vaccination programs may be necessary to facilitate the ambitious objective of eradicating measles from Nepal.

Declaration of competing interest

The authors declare that they have no known competing financial interests or personal relationships that could have appeared to influence the work reported in this paper.

Authors declare

No conflict of interest.

CRediT authorship contribution statement

Anjana Pokharel: Writing – original draft, Methodology, Investigation, Formal analysis. **Khagendra Adhikari:** Writing – original draft, Methodology, Investigation, Formal analysis. **Ramesh Gautam:** Writing – original draft, Methodology, Investigation, Formal analysis. **Kedar Nath Uprety:** Writing – review & editing, Supervision, Formal analysis. **Naveen K. Vaidya:** Writing – review & editing, Supervision, Formal analysis, Conceptualization.

Acknowledgments

This research is supported by the GRAID (Graduate Research Assistantships in Developing Countries) awards from the International Mathematical Union (IMU). AP acknowledges the University Grants Commission (UGC), Sanothimi Bhaktapur, Nepal, for the Small Research and Development and Innovation Grants-077/078 (SRDIG) award. KA acknowledges the Nepal Academy of Science and Technology (NAST) for Ph.D. Fellowship. RG acknowledges the University Grants Commission (UGC) Nepal for Ph.D. Fellowship 2021. The work of NKV was supported by NSF grants DMS-1951793 and DEB-2030479 from the National Science Foundation of USA and UGP award from San Diego State University.

Appendix A. Supplementary data

Supplementary data to this article can be found online at https://doi.org/10.1016/j.idm.2024.04.012.

References

Adhikari, K., Gautam, R., Pokharel, A., Dhimal, M., Uprety, K. N., & Vaidya, N. K. (2022). Insight into delta variant dominated second wave of covid-19 in Nepal. *Epidemics, 41*, Article 100642. https://doi.org/10.1016/j.epidem.2022.100642

Adhikari, K., Gautam, R., Pokharel, A., Uprety, K. N., & Vaidya, N. K. (2021). Transmission dynamics of covid-19 in Nepal: Mathematical model uncovering effective controls. *Journal of Theoretical Biology, 521*, Article 110680. https://doi.org/10.1016/j.jtbi.2021.110680

Castillo-Chávez, C., Zhilan, F., & Huang, W. (2002). On the computation of r0 and its role in global stability. *IMA Volumes in Mathematics and its Applications, 125*, 229–250. https://doi.org/10.1007/978-1-4757-3667-0_13

Dall, C. (2023). *Nepal hit by measles outbreak*. URL https://www.who.int/emergencies/disease-outbreak-news/item/2023-DON446.

Diekmann, O., & Heesterbeek, J. A. P. (2001). Mathematical epidemiology of infectious diseases: Model building, analysis and interpretation. *International Journal of Epidemiology, 30*(1), 186. https://doi.org/10.1093/ije/30.1.186, 186.

Diekmann, O., Heesterbeek, J. A. P., & Roberts, M. G. (1992). Seroepidemiology and evaluation of passive surveillance during 1988–1989 measles outbreak in Taiwan. *International Journal of Epidemiology, 21*(6), 1165–1174. https://doi.org/10.1098/rsif.2009.0386

Dipo, A., & Dinda, A. (2019). A deterministic model of measles with imperfect vaccination and quarantine intervention. *International Conference on Mathematics: Pure, Applied and Computation, 1218*. https://doi.org/10.1088/1742-6596/1218/1/012044, 012044–012054.

Edward, S., Kitengeso Raymond, E., Kiria Gabriel, T., Nestory, F., Mwema, G., Godfrey, P., et al. (2015). A mathematical model for control and elimination of the transmission dynamics of measles. *Applied and Computational Mathematics, 4*, 396–408. https://doi.org/10.11648/j.acm.20150406.12

Farman, M., Shehzad, A., Akgül, A., Baleanu, D., & Sen, M. D.l. (2023). Modelling and analysis of a measles epidemic model with the constant proportional caputo operator. *Symmetry, 15*(2). https://doi.org/10.3390/sym15020468

Garba, S. M., Safi, M. A., & Usaini, S. (2017). Mathematical model for assessing the impact of vaccination and treatment on measles transmission dynamics. *Mathematical Methods in the Applied Sciences, 40*(18). https://doi.org/10.1002/mma.4462

Gautam, R., Pokharel, A., Adhikari, K., Uprety, K. N., & Vaidya, N. K. (2022). Modeling malaria transmission in Nepal: Impact of imported cases through cross-border mobility. *Journal of Biological Dynamics, 16*(1), 528–564. https://doi.org/10.1080/17513758.2022.2096935

Haileyesus, T. A., & Asnakew, M. B. (2023). Modelling, analysis, and simulation of measles disease transmission dynamics. *Discrete Dynamics in Nature and Society, 2023*. https://doi.org/10.1155/2023/9353540

Ichimura, Y., Yamauchi, M., Yoshida, N., Miyano, S., Komada, K., Thandar, M., et al. (2022). *Effectiveness of immunization activities on measles and rubella immunity among individuals in east sepik, Papua New Guinea: A cross-sectional study, PMC- IJID 3*. https://doi.org/10.1016/j.ijregi.2022.03.001

Jaharuddin, B. T. (2020). Control policy mix in measles transmission dynamics using vaccination, therapy, and treatment. *International Journal of Mathematics and Mathematical Sciences, 2020*, 20. https://doi.org/10.1155/2020/1561569

Joshi, A. B. (2009). Measles deaths in Nepal: Estimating the national cases in fatality ratio. *Bulletin of the World Health Organization, 87*(6), 405–484. https://doi.org/10.2471/BLT.07.050427, 2009.

Khanal, et al. (2016). Progress toward measles elimination — Nepal, 2007–2014. *CDC Morbidity and Mortality Weekly Report (MMWR), 65*(8), 206–210. https://doi.org/10.15585/mmwr.mm6508a3externalicon

Kuddus, M., Mohiuddin, M., & Rahman, A. (2021). Mathematical analysis of a measles transmission dynamics model in Bangladesh with double dose vaccination. *Scientific Reports, 11*(1), Article 16571. https://doi.org/10.1038/s41598-021-95913-8

Kumar, S. S., Hartner, A.-M., Chandran, A., Gaythorpe, K. A. M., Li, X., et al. (2023). Evaluating effective measles vaccine coverage in the malaysian population accounting for between-dose correlation and vaccine efficacy. *BMC Public Health, 23*(2351). https://doi.org/10.1186/s12889-023-17082-9

Lessler, J., Metcalf, C., Cutts, F., & Grenfell, B. (2016). Impact on epidemic measles of vaccination campaigns triggered by disease outbreaks or serosurveys: A modeling study. *PLoS Medicine, 13*(10). https://doi.org/10.1371/journal.pmed.1002144

Lochlainn, L. N., de Gier, B., van der Maas, N., Strebel, P., Goodman, T., van Binnendijk, R., et al. (2019). Immunogenicity, effectiveness, and safety of measles vaccination in infants younger than 9 months: A systematic review and meta-analysis. *The Lancet Infectious Diseases, 11*. https://doi.org/10.1016/S1473-3099(19)30395-0, 1235–124.

Macrotrends, Nepal population 1950-2020. URL https://www.macrotrends.net/countries/NPL/nepal/population.

Meredith, G. D., Matt, F., Sebastien, A., Xi, L., Allison, P., Brian, L., et al. (2021). Progress toward regional measles elimination worldwide, 2000–2020. *Morbidity and Mortality Weekly Report, 70*(45).

Min-Shi, L., Chwan-Chuen, K., Jia-Yuh, J., Chuan-Liang, K., Chen, W. C., Mei-Shang, H., et al. (2009). The construction of next-generation matrices for compartmental epidemic models. *International Journal of Epidemiology*, (7), 1165–1174. https://doi.org/10.1098/rsif.2009.0386

Motulasky, H., & Arthur, C. (2003). *Fitting model to biological data using linear and non linear regression. A practical guide to curve fitting*. San Diego,CA: Graph Pad Software Inc. URL www.graphpad.com.

Mutua, J. M., Wang, F.-B., & Vaidya, N. K. (2015). Modeling malaria and typhoid fever co-infection dynamics. *Mathematical Biosciences, 264*, 128–144. https://doi.org/10.1016/j.mbs.2015.03.014

N. S. Office. (2021). *National population and housing census* (national report). URL https://censusnepal.cbs.gov.np/results.

Pantha, B., Giri, S., Joshi, H., & Vaidya, N. K. (2021). Modeling transmission dynamics of rabies in Nepal. *Infect. Dis. Model, 6*, 284–301. https://doi.org/10.1016/j.idm.2020.12.009

Peter, O. J., Fahrani, N. D., Fatmawati, W., & Chukwu, C. (2023). A fractional derivative modeling study for measles infection with double dose vaccination. *Healthcare Analytics, 4*, Article 100231. https://doi.org/10.1016/j.health.2023.100231

Peter, O. J., Ojo, M. M., Viriyapong, R., & Oguntolu, F. A. (2022). Mathematical model of measles transmission dynamics using real data from Nigeria. *Journal of Difference Equations and Applications, 28*(6), 753–770. https://doi.org/10.1080/10236198.2022.2079411

Peter, O. J., Qureshi, S., Ojo, M. M., Viriyapong, R., & Soomro, A. (2023). Mathematical dynamics of measles transmission with real data from Pakistan. *Model. Earth Syst. Environ, 9*, 1545–1558. https://doi.org/10.1007/s40808-022-01564-7

Pokharel, A., Adhikari, K., Gautam, R., Uprety, K. N., & Vaidya, N. K. (2022). Modeling transmission dynamics of measles in Nepal and its control with monitored vaccination program. *Mathematical Biosciences and Engineering, 19*(8). https://doi.org/10.3934/mbe.2022397

Poudel, A. (2019). *Low vaccine coverage rate, floating population leading to repeat measles outbreaks*. URL https://reliefweb.int/report/nepal/low-vaccine-coverage-rate-floating-population-leading-repeat-measles-outbreaks.

Roberts, T. M. M. (2000). Predicting and preventing measles epidemics in New Zealand. *Epidemiology and Infection, 124*, 279–287. https://doi.org/10.1017/S0950268899003556

Sekhar, B. A., Rai, P., Gupta, B. P., Pradhan, R., Lacoul, M., Shakya, S., et al. (2022). Nepal measles outbreak response immunization during covid-19: A risk-based intervention strategy. *Vaccine, 40*(20), 2884–2893.

MoHP, 2024. Government of Nepal, Ministry of Health and Population, National Immunization Programme. URL https://mohp.gov.np/program/national-immunisation-programme/en.

Simeone, M., Hogue, I. B., Ray, C. J., & Kirschner, D. E. (2008). A methodology for performing global uncertainty and sensitivity analysis in systems biology. *Journal of Theoretical Biology, 254*(1), 178–196. https://doi.org/10.1016/j.jtbi.2008.04.011

Song, X., Jiang, Y., & Wei, H. (2019). Analysis of a saturation incidence SVEIRS epidemic model with pulse and two time delay. *Applied Mathematics and Computation, 214*. https://doi.org/10.1016/j.amc.2009.04.005

Statista. (2023). *Share of children in total population in Nepal from 2013 to 2022*. URL https://www.statista.com/statistics/678090/nepal-children-as-a-percentage-of-the-population/.

Thakur, C. K., Gupta, N., Pokhrel, N., Adhikari, S., Dhimal, M., & Gyanwali, P. (2024). Stumbling blocks on the path to measles-free Nepal: Impact of the covid-19 pandemic. *Tropical Medicine and Health, 52*(10). https://doi.org/10.1186/s12889-023-17082-9

Trottier, H., & Philippe, P. (2000). Deterministic modeling of infectious diseases: Theory and methods. *The Internet Journal of Infectious Diseases, 1*(2). https://doi.org/10.1016/S0031-8914(53)80099-6

Truong, T., Mulders, A. N., Gautam, M. C., Ammerlaan W, D. L., de Swart, R., King, C., et al. (2001). Genetic analysis of Asian measles virus strains—new endemic genotype in Nepal. *Virus Research, 76*(1), 71–78. https://doi.org/10.1016/s0168-1702(01)00255-6

Unicef for Every Child, More than 140,000 die from measles as cases surge worldwide. (2019). URL https://www.who.int/news/item/05-12-2019-more-than-140-000-die-from-measles-as-cases-surge-worldwide#:?:text=Worldwide%20more%20than%20140%2C000%20people,devastating%20outbreaks%20in%20all%20regions.

Vaidya, N. K., & Wang, F.-B. (2022). Persistence of mosquito vector and dengue: Impact of seasonal and diurnal temperature variations, Discrete and Continuous Dynamical Systems - B. *27*(1), 393–420. https://doi.org/10.3934/dcdsb.2021048

van den Driessche, P., & Watmough, J. (2002). Reproduction numbers and sub-threshold endemic equilibria for compartmental models of disease transmission. *Mathematical Biosciences, 180*. https://doi.org/10.1016/S0025-5564(02)00108-6

WHO. (2020). *Measles and rubella strategic framework 2021–2030*. URL https://www.who.int/publications/i/item/measles-and-rubella-strategic-framework-2021-2030.

WHO. (2022). *Nearly 40 million children are dangerously susceptible to growing measles threat*. URL https://www.who.int/news/item/23-11-2022-nearly-40-million-children-are-dangerously-susceptible-to-growing-measles-threat.

WHO. (2023a). *Measles*. URL https://www.who.int/news-room/fact-sheets/detail/measles.

WHO. (2023b). *Measles vaccination coverage*. URL https://immunizationdata.who.int/pages/coverage/MCV.html?CODE=Global+NPL&ANTIGEN=MCV1&YEAR=.

WHO. (2023c). *Measles reported cases and incidence*. URL https://immunizationdata.who.int/pages/incidence/MEASLES.html?CODE=Global+NPL&YEAR=.

WHO. (2023d). *Measles-Nepal*. URL https://www.cidrap.umn.edu/measles/nepal-hit-measles-outbreak.

WHO-Measles. (2019). *Towards elimination in Nepal*. URL https://www.who.int/southeastasia/news/feature-stories/detail/measles-towards-elimination-in-nepal.

World Health Organization. (2023a). *Measles - Nepal*. URL https://www.who.int/emergencies/disease-outbreak-news/item/2023-DON446.

World Health Organization. (2023b). *Measles*. URL https://www.who.int/news-room/fact-sheets/detail/measles.